Applied Physics Letters

Single-mode operation of terahertz quantum cascade lasers with distributed feedback resonators

Cite as: Appl. Phys. Lett. **84**, 5446 (2004); https://doi.org/10.1063/1.1767957
Submitted: 05 February 2004 • Accepted: 07 May 2004 • Published Online: 17 June 2004

Lukas Mahler, Rüdeger Köhler, Alessandro Tredicucci, et al.

View Online Export Citation

ARTICLES YOU MAY BE INTERESTED IN

Thermoelectrically cooled THz quantum cascade laser operating up to 210 K
Applied Physics Letters **115**, 010601 (2019); https://doi.org/10.1063/1.5110305

High-performance operation of single-mode terahertz quantum cascade lasers with metallic gratings
Applied Physics Letters **87**, 181101 (2005); https://doi.org/10.1063/1.2120901

Coupled-Wave Theory of Distributed Feedback Lasers
Journal of Applied Physics **43**, 2327 (1972); https://doi.org/10.1063/1.1661499

© 2004 American Institute of Physics.

HTML ABSTRACT + LINKS

Single-mode operation of terahertz quantum cascade lasers with distributed feedback resonators

Lukas Mahler,[a] Rüdeger Köhler,[b] Alessandro Tredicucci, and Fabio Beltram
NEST-INFM and Scuola Normale Superiore, Piazza dei Cavalieri 7, 56126 Pisa, Italy

Harvey E. Beere, Edmund H. Linfield, and David A. Ritchie
Cavendish Laboratory, University of Cambridge, Madingley Road, Cambridge CB3 0HE, United Kingdom

A. Giles Davies
School of Electronic and Electrical Engineering, University of Leeds, Leeds LS2 9JT, United Kingdom

(Received 5 February 2004; accepted 7 May 2004; published online 17 June 2004)

Distributed feedback terahertz quantum-cascade lasers emitting at 4.34 and 4.43 THz are presented. Mode selection is based on a complex-coupling scheme implemented into the top-contact layer by a combination of wet chemical etching and ohmic-contact deposition. Single-mode emission stable at all injection currents and operating temperatures is shown, with a side-mode suppression ratio exceeding 20 dB. Peak output powers of up to 1.8 mW are obtained at low temperatures. © *2004 American Institute of Physics*. [DOI: 10.1063/1.1767957]

The terahertz region (1–10 THz) of the electromagnetic spectrum has long been of great interest in astronomical and atmospheric sensing. Over the past decade several applications such as tomography, biological analysis, and chemical monitoring have evolved. Progress in these areas, however, has been hampered by the lack of compact, convenient sources providing narrow-band, tunable emission. Recently, terahertz semiconductor lasers[1] based on the quantum cascade (QC) principle[2] were realized, and very promising performance has since been demonstrated.[3–5] These lasers employ a multimode Fabry–Pérot cavity; therefore, single-mode operation is observed only occasionally with very short resonators and over a limited range of injection currents.[3,6] Stable single-mode emission at a precisely designed frequency is, however, highly desirable for most applications. This has been achieved in conventional interband lasers and in mid-infrared QC lasers by using distributed feedback (DFB) resonators;[7] indeed QC-DFB lasers[8] are now becoming widely employed in spectroscopy and sensing.[9] Here, we report the realization of terahertz QC-DFB lasers showing well-defined, consistent single-mode emission with a side-mode suppression ratio of better than 20 dB.

Unlike in mid-infrared QC-DFB lasers, which employ a dielectric waveguide, the waveguide of far-infrared ($\lambda \sim 17-24\ \mu$m)[10–12] and terahertz QC lasers ($\lambda \sim 65-106\ \mu$m)[1,4,6,13,14] relies on the formation of surface plasmons. These optical modes propagate along the interface between materials with dielectric constants of opposite sign, and decay exponentially perpendicular to the interface, with a skin depth controlled by the relevant dielectric constants. At far-infrared wavelengths, this allows the implementation of DFB directly into the top contact by producing a grating of two different metals, which causes a modulation of the complex refractive index.[10] Unfortunately, at terahertz frequencies, all common metals become very much like perfect conductors, owing to the very high values of the plasma frequencies, leading to a very weak accessible modulation. Yet, the peculiar structure of terahertz QC[1] waveguides still makes it possible to implement this scheme. In fact, the low-doped stack of active regions is sandwiched between a bottom contact layer and a top contact layer/metallization. While doping and thickness of the bottom contact layer are engineered to control the mode profile and its penetration into the substrate, the semiconductor top contact layer (typically, 200 nm GaAs, doped to $n=5\times10^{18}$ cm^{-3}) does not contribute substantially to waveguiding. Its thickness is much smaller than radiation penetration depth and, consequently, the laser mode is driven mainly by the top gold metallization. The influence of the doped GaAs layer is through its impact on mode boundary conditions and the ensuing effect on propagation coefficients. Plasmon energy in such semiconductor layers is less than 100 meV, much lower than that of gold. An effective refractive index modulation can therefore be created by patterning a grating *into* the GaAs layer. Figure 1 shows a computation of the vertical profile of the guided mode for a laser structure identical to that of Ref. 3. Together with the unperturbed waveguide, results are also reported for the cases where the thickness of the top contact layer was reduced to 50 nm or the latter was entirely removed. The mode profiles were calculated using a Drude model for the refractive indices of the semiconductor layers, and solving Helmholtz equations for a slab waveguide model. For the unperturbed region we find $n_{\mathrm{eff}}=3.728$ at an emission wavelength of 147 cm^{-1}; in the region of 50 nm top layer thickness we find $n_{\mathrm{eff}}=3.739$. There is also a modulation of the propagation losses $\Delta\alpha_W=1.5$ cm^{-1} and of the modal gain $g_{th}\Delta\Gamma=1.3$ cm^{-1}. While the mode in the regions of reduced top layer thickness experiences lower gain, it also has lower losses. As a result, the DFB is essentially purely index-coupled. If we compute the coupling constant considering just the difference in n_{eff} of the two modes we obtain $k=\pi\Delta n_{\mathrm{eff}}/(4n_{\mathrm{eff}}\Lambda)=2.5$ cm^{-1}. This value may, however, be an underestimate since it does not take into account the strong modulation of the spatial mode profiles shown in Fig. 1. In fact, the latter introduces an impedance mismatch between the modes existing in the crest and trough regions of the grating. The values of n_{eff} are anyway highly

[a]Also with: Department of Physics, ETH Zurich, CH-8093 Zurich, Switzerland.
[b]Electronic mail: koehler@sns.it

 © 2004 American Institute of Physics

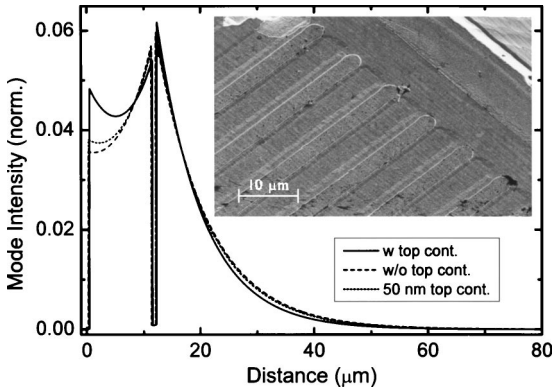

FIG. 1. Calculated mode profiles of the waveguide for different thicknesses of the top contact layer: 200 nm (solid line), 50 nm (dotted line), and after complete removal of the layer (dashed line). With decreasing layer thickness, the mode is pushed further into the substrate causing a modulation of the complex effective refractive index. The inset shows a microscope image of a 9.2 μm grating etched to a depth of 220 nm, i.e., following complete removal of the top contact layer. Annealed Au/GeAu ohmic contacts, which are deposited on the crests of the grating, appear brighter than the GaAs surface. On the upper right part of the figure the edge of the ridge is visible.

sensitive to the choice of carrier–carrier scattering times and static dielectric constants in the calculation. It should also be noted that, owing to the large spectral dispersion, the group refractive index of 4.14 inferred from the mode spacing in the Fabry–Pérot spectra (see Fig. 2) differs substantially from the effective refractive index needed to compute the correct grating period. Moreover, since the spectral width of the gain $\Delta\nu$ does not exceed ≈ 6 cm^{-1}, even small variations in the refractive index lead to a substantial detuning of gain and grating resonance. Consequently, in order to account for these uncertainties, a set of devices was fabricated with grating periods from $\Lambda = 8.6$ to 9.8 μm (steps of 200 nm) corresponding, for nearly 50% duty-cycle, to average refractive

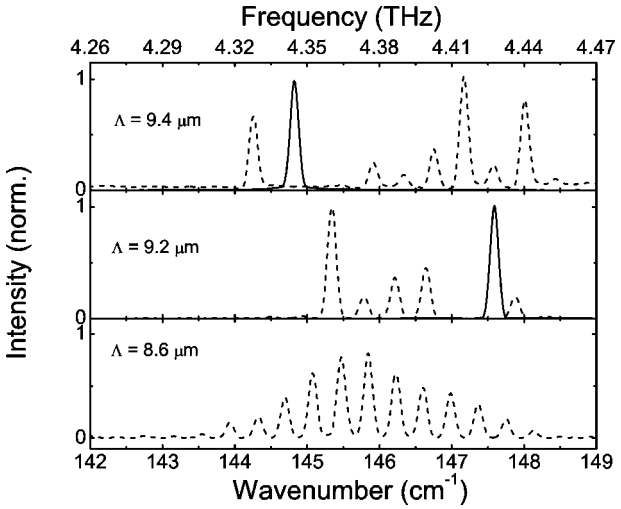

FIG. 2. Spectra of five different lasers with grating periods of 9.4, 9.2, and 8.6 μm, respectively, collected at an injection current close to the maximum output power. In the upper two panels, dashed lines correspond to spectra recorded from devices in which the distributed feedback was implemented only by removing 150 nm of the top contact layer. The appearance of a stop-band in the original Fabry–Pérot spectrum indicates a predominant index-modulation. Solid lines are spectra recorded from devices in which an additional loss-modulation was introduced by an annealed-contact grating (see text). In this case, the stronger modulation leads to stable single-mode emission. In the bottom panel, the spectrum of a 150 nm etched device with no annealed-contact grating and $\Lambda = 8.6$ μm is shown.

indices of 3.95 to 3.47. Samples were processed from a nominally identical replica of the original heterostructure described in Ref. 1, first introducing a periodic corrugation by wet chemical etching to a depth of 150 nm, then following the protocol described in Ref. 3. Laser bars were cleaved, soldered onto copper blocks, and mounted on the cold finger of a liquid-helium cryostat. The experimental apparatus is identical to that of Ref. 3: Spectra were recorded using a Fourier-transform infrared spectrometer in rapid scan mode with a resolution of 0.125 cm^{-1}, driving the lasers at duty cycles between 1 and 10%, and using either a He-cooled bolometer or a DTGS pyroelectric for detection.

Figure 2 shows five spectra recorded from devices of length $L_c = 2.8$ mm with grating periods Λ equal to 8.6, 9.2, and 9.4 μm, respectively. For $\Lambda - 8.6$ μm, a nearly perfect Fabry–Pérot spectrum, shown in the bottom panel, is obtained, indicating either an insufficient coupling strength or a large detuning of the grating resonance with respect to the laser gain. In the two devices with $\Lambda = 9.2$, 9.4 μm, again a regularly spaced Fabry–Pérot spectrum is observed (dashed lines), but two modes are strongly suppressed. This is a typical feature of index-coupled DFB lasers with only moderate coupling strength but strong reflectivity at the Fabry–Pérot facets.[15] Small values of $k \cdot L$ considerably increase the threshold gain for two of the original Fabry–Pérot modes centered around the grating resonance, while the modes left and right of this stop-band experience a lower threshold, but with weak selectivity. Moreover, in the case of small $k \cdot L$, the mode spacing of the lasing modes remains almost unchanged with respect to the Fabry–Pérot spacing. For this reason, the stop-band width cannot be used to derive a measurement of the coupling constant. The spectral position of the stop-band, however, is in fair agreement with the average effective refractive index from our simulation, and the position shifts precisely with the grating period.

The large number of Fabry–Pérot modes observed at high current excitation could also be related to spatial hole burning in these devices. In fact, the optical power inside the resonator is close to the saturation intensity I_s,[16] which, in our case, is estimated of the order of few kW/cm^2. A detailed theoretical analysis[17] predicts that in index-coupled lasers the mode selectivity in the vicinity of the saturation decreases strongly with increasing output power owing to the additional "gain grating" arising from spatial hole burning. In contrast, gain-coupled DFB lasers are found to be much less sensitive to this effect.

In order to enhance the coupling constant we increased the corrugation depth of the grating to 220 nm. Furthermore, to increase mode discrimination and reduce the extent of possible spatial hole burning effects, an additional loss modulation was introduced by depositing and annealing GeAu/Au contacts[3] selectively on the crests of the grating (inset: Fig. 1). By comparing devices with an annealed contact across the entire ridge[1] and devices, where only two narrow ridges have been contacted,[3] this further processing step is estimated to introduce a difference in waveguide losses of ~ 8 cm^{-1}. Thus, complex-coupled DFB resonators, which are much more effective in achieving single-mode operation than bare index-coupled devices, are obtained with an estimated coupling constant of 4 cm^{-1}. Devices were accordingly fabricated with grating periods of 9.2 and 9.4 μm. No other changes were introduced in the fabrication process. Figure 2 shows the spectra (solid lines) of two such devices

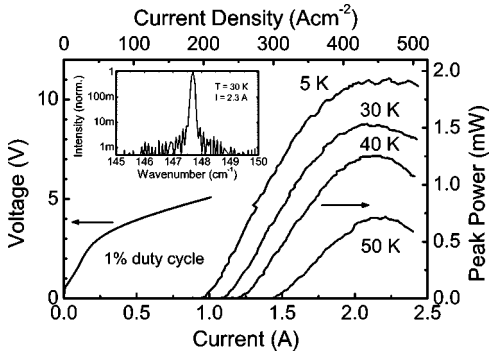

FIG. 3. Light-current and voltage-current characteristics of a 3.2 mm long and 150 μm wide laser with a grating period of 9.2 μm, collected at heat sink temperatures of 5, 30, 40, and 50 K. Values represent the power collected (efficiency 33%) from one laser facet by the bolometer after correction for the transmittance of the polyethylene window (0.63). Lasing ceases at 55 K. The voltage-current characteristics are similar to those of devices processed with the standard protocol, indicating no problems with electrical contacting. The inset shows an example laser spectrum recorded at 30 K under an injection current of 2.3 A. A side-mode suppression of more than 20 dB is obtained; the linewidth of the laser is limited by the resolution of the experimental apparatus (0.125 cm^{-1}=3.75 GHz).

(length 3.2 mm and Λ=9.2 μm in one device and 4.4 mm with Λ=9.4 μm in the other). Lasing takes place within the previously observed stop band, as expected for a complex-coupled DFB laser. Again, the shift of the emission wavelength corresponds precisely to the change of grating period, and an effective refractive index of 3.68 can be extracted, in good agreement with the calculated value of 3.73. The coupling is now sufficiently strong to achieve single-mode operation under all injection currents and operating temperatures. An example high-resolution spectrum plotted on a logarithmic scale is shown in the inset of Fig. 3. The power of this laser mode exceeds that of the remaining Fabry–Pérot modes by a factor of at least 100, i.e., a side-mode suppression ratio exceeding 20 dB is obtained. Several devices were measured and identical characteristics found. The variation in emission wavelength between different devices with nominally identical grating periods was not more than 0.4 cm^{-1}, and could be attributed to slight variations in the effective refractive index. The tuning of emission wavelength with temperature and current is below the resolution of the experimental apparatus. However, in Fabry–Pérot devices, a tuning coefficient of 4 MHz/mA was observed and an instantaneous linewidth of 30 kHz was measured with a 3 ms sweep, using an unstabilized power supply.[18] While we can expect a similar tuning coefficient for our device, the emission linewidth of a DFB laser is typically well below that of a Fabry–Pérot cavity.

Figure 3 shows the light-current characteristics of the 3.2 mm long device (Λ=9.2 μm) for different operating temperatures, collected at a duty cycle of 1%. Almost 2 mW of peak power is obtained at 5 K, and still 700 μW is emitted at 50 K. Lasing ceases around 55 K. The threshold current density at 5 K is 200 A cm^{-2}, slightly higher than in Fabry–Pérot lasers, where thresholds between 160 and 180 A/cm^2 were obtained from the same sample growth.[3] Likewise, the slope efficiency of 13 mW/A at 5 K, measured as the change in output power with inejction current from threshold to 1.5 A, is lower for the DFB lasers. This is most likely a result of the higher waveguide losses caused by the loss modulation, but could also be linked to the concentration of the emitted power close to the center of the device caused by the large coupling constant.[7] Assuming an increase in the average waveguide losses of 4 cm^{-1} and a reduction of the outcoupling loss owing to the longer device and the DFB, this compares well to the 25 mW/A observed in lasers with a Fabry–Pérot cavity.[3] These characteristics indicate that the introduction of the gratings does not lower device performance substantially.

In summary, we have demonstrated stable single-mode emission with side-mode suppression ratios of better than 20 dB in THz QC-DFB lasers. The single-mode emission was achieved by implementing a complex-coupling scheme based on a combination of wet chemical etching and deposition of annealed ohmic contacts on the topmost layer of the heterostructure. This result should further accelerate the implementation of terahertz QC lasers in many spectroscopic applications with particular relevance to astronomical and atmospheric sensing.

This work was supported in part by the European Commisson through the IST Frame-work V FET project WANTED. R.K. and A.T. acknowledge support by the Fondazione Cassa di Risparmio di Pisa and by Physical Sciences Inc.; E.H.L. acknowledges support from Toshiba Research Europe Ltd.

[1] R. Köhler, A. Tredicucci, F. Beltram, H. E. Beere, E. H. Linfield, A. G. Davies, D. A. Ritchie, R. C. Iotti, and F. Rossi, Nature (London) **417**, 156 (2002).
[2] J. Faist, F. Capasso, D. L. Sivco, C. Sirtori, A. L. Hutchinson, and A. Y. Cho, Science **264**, 553 (1994).
[3] R. Köhler, A. Tredicucci, F. Beltram, H. E. Beere, E. H. Linfield, A. G. Davies, D. A. Ritchie, S. Dhillon, and C. Sirtori, Appl. Phys. Lett. **82**, 1518 (2003).
[4] G. Scalari, L. Ajili, J. Faist, H. E. Beere, E. H. Linfield, D. A. Ritchie, and A. G. Davies, Appl. Phys. Lett. **82**, 3165 (2003).
[5] B. S. Williams, S. Kumar, H. Callebaut, Q. Hu, and J. L. Reno, Appl. Phys. Lett. **83**, 5142 (2003).
[6] R. Köhler, A. Tredicucci, F. Beltram, H. E. Beere, E. H. Linfield, A. G. Davies, and D. A. Ritchie, Opt. Lett. **28**, 810 (2003).
[7] H. Kogelnik and C. V. Shank, J. Appl. Phys. **43**, 2327 (1972).
[8] T. Aellen, S. Blaser, M. Beck, D. Hofstetter, and J. Faist, Appl. Phys. Lett. **83**, 1929 (2003).
[9] F. K. Tittel, A. A. Kosterev, M. Rochat, M. Beck, and J. Faist, Proc. SPIE **4817**, 8 (2002).
[10] A. Tredicucci, C. Gmachl, F. Capasso, A. L. Hutchinson, D. L. Sivco, and A. Y. Cho, Appl. Phys. Lett. **76**, 2164 (2000).
[11] A. Tredicucci, C. Gmachl, M. C. Wanke, F. Capasso, A. L. Hutchinson, D. L. Sivco, S. N. G. Chu, and A. Y. Cho, Appl. Phys. Lett. **77**, 2286 (2000).
[12] R. Colombelli, F. Capasso, C. Gmachl, A. L. Hutchinson, D. L. Sivco, A. Tredicucci, M. C. Wanke, A. M. Sergent, and A. Y. Cho, Appl. Phys. Lett. **78**, 2620 (2001).
[13] B. S. Williams, H. Callebaut, S. Kumar, Q. Hu, and J. L. Reno, Appl. Phys. Lett. **82**, 1015 (2003).
[14] R. Köhler, A. Tredicucci, F. Beltram, H. E. Beere, E. H. Linfield, D. A. Ritchie, and A. G. Davies, Electron. Lett. **39**, 1254 (2003).
[15] W. Streifer, R. D. Burnham, and D. R. Scifres, IEEE J. Quantum Electron. **11**, 154 (1975).
[16] A. Yariv, *Optical Electronics in Modern Communications*, 5th ed. (Oxford UP, Oxford, 1997).
[17] W. S. Rabinovich and B. J. Feldmann, IEEE J. Quantum Electron. **20**, 25 (1989).
[18] A. Barkan, F. K. Tittel, D. M. Mittleman, R. Dengler, P. Siegel, G. Scalari, L. Ajili, J. Faist, H. E. Beere, E. H. Linfield, A. G. Davies, and D. A. Ritchie, Opt. Lett. **29**, 575 (2004).